Research in Astron. Astrophys. **2012** Vol. **12** No. **1**, 46–62
http://www.raa-journal.org *http://www.iop.org/journals/raa*

***R**esearch in*
***A**stronomy and*
***A**strophysics*

Model-fitting of the kinematics of superluminal components in blazar 3C 279

Shan-Jie Qian

National Astronomical Observatories, Chinese Academy of Sciences, Beijing 100012, China;
rqsj@bao.ac.cn

Received 2011 April 30; accepted 2011 August 23

Abstract A precessing jet-nozzle model with a precession period of about 25 yr has been proposed by Qian to interpret the change with time of the ejection position angle of the superluminal components observed using very long baseline interferometry (VLBI) in the blazar 3C 279. We discuss the kinematic properties of six superluminal knots (C3, C4, C7a, C8, C9 and C10) and show that their trajectory, core-distance and apparent speed, derived from VLBI observations, can be consistently well fitted by the model. Their intrinsic Lorentz factors of bulk superluminal motion are thus derived, and the evidence shows no relation between Lorentz factor and the precession phase. Interestingly, for the C7a and C8 knots, the fitted core-distance ranges from $\sim$0.1 mas to $\sim$0.4 mas and for knots C9 and C10 from $\sim$0.2 mas to $\sim$1.0–1.5 mas. For knot C4, its trajectory and apparent velocity are well fitted in the core-distance range from $\sim$1 mas to $\sim$5 mas, taking into account a curvature of the trajectory at core-distance larger than $\sim$3 mas. The consistent fitting of the kinematics of these components clearly demonstrates that the amplitude function and collimation parameter adopted in the precession model are appropriate and applicable for both the inner and outer parts of the jet in 3C 279, but in some cases the jet curvature in the outer parts (or deviation from the model trajectory) needs to be seriously taken into consideration. With the exception of C4, the ejection position angles derived from the precession model are consistent with the values measured by VLBI observations (within about $3^\circ - 6^\circ$). Undoubtedly, the consistent interpretation of the kinematics in terms of the precession model for these superluminal components, with their ejection time spanning $\sim$24 yr, significantly expands its applicability and implies that regular patterns of trajectories (or rotating channels) could exist in some periods.

Key words: radio continuum — galaxies: jets — galaxies: kinematics — galaxies: individual (blazar 3C 279)

1 INTRODUCTION

Research on blazars is an important extragalactic astrophysical field, in which extensive observations of their radiation from radio to γ-ray are carried out, and the mechanisms of radiation are studied (recent progress can be seen in Marscher et al. 2011; Marscher & Jorstad 2011; Abdo et al. 2010; Jorstad et al. 2010; Agudo et al. 2011; Raiteri et al. 2010; Schinzel et al. 2010; Vercellone et al. 2010; Marscher et al. 2010; Qian 2011). 3C 279 ($z = 0.538$) is an archetypal source and one of the most well studied prominent blazars (flat-spectrum compact radio sources with superluminal motion). It has an optically violent variable (OVV) with large and rapid polarized outbursts and radiates across the entire electromagnetic spectrum from radio through optical and X-ray to γ-ray. Very strong variability is observed in all these wavebands with various timescales (hours/days to years). 3C 279 is one of the brightest EGRET quasars (Hartman et al. 1992). Multifrequency observations and the study of correlations between different wavebands have demonstrated important clues to the radiation mechanisms, especially for X-ray and γ-ray radiation and their emission positions in the jet (Jorstad et al. 2007; Marscher 2008, 2009; Marscher & Jorstad 2011; Marscher et al. 2011).

3C 279 is the first object in which superluminal motion was detected (Whitney et al. 1971; Cohen et al. 1971). Since then, its mas-scale (milli-arc-second scale) structure and kinematics have been monitored using very long baseline interferometry (VLBI). Numerous amounts of data have been presented in the literature on the kinematics and flux-polarization evolution of superluminal knots. VLBI observations reveal that bright components (knots) are consistently ejected from a core (presumed to be stationary) and move away from it with apparent superluminal speeds ($\sim$4–16 c, Chatterjee et al. 2008; Larionov et al. 2008; Jorstad & Marscher 2005; Jorstad et al. 2004; Homan et al. 2003; Wehrle et al. 2001; Carrara et al. 1993; Unwin et al. 1989). Apparent superluminal motion results from relativistic motion of the components at small viewing angles and their flux density or luminosity is strongly Doppler-boosted. Thus the determination of their intrinsic flux (luminosity) and variation is only possible when their Doppler factor is measured (Qian et al. 1996; Steffen et al. 1995).

In the previous paper (Qian 2011), a jet-nozzle precession model with a precession period of $\sim$25 yr has been proposed to interpret the change with time of the ejection position angle of the superluminal knots of blazar 3C 279. With VLBI data collected from literature spanning about 30 yr we show that the ejection position angles observed can be well fitted by the model for a number of the knots, including, for example, C3, C4 and even C24. The main features of the model are:

(1) The position angle derived by the model ranges between $\sim -155°$ and $\sim -80°$.
(2) The model gives small viewing angles for all the superluminal knots, between $\sim$0.5° and $\sim$2°.
(3) A precession period of 25 yr can be applied to fit the initial (ejection) position angles observed for knots C3, C4, C5 and C24, etc, covering a time interval beyond one period.
(4) In particular, the model provides a good fit to the trajectory of knot C4 within a core-distance $\leq$3 mas, showing that its initial ejection position angle can be derived from the model and is consistent with the precession phase corresponding to its ejection epoch.

These features can be summarily described using Figures 1 and 2 and Table 1. In Table 1 the precession phase ϕ, ejection epoch and initial (ejection) position angle of the 25-year precession model are given. Figure 1 shows the distribution of the trajectory. Figure 2 shows the relationship of the ejection position angle with the precession phase (a) and the relation between the initial viewing angle and the initial position angle (b), showing the rotation of the trajectory.

In the following we will study in detail the kinematics of six superluminal components (C3, C4, C7a, C8, C9 and C10) and show that their trajectory and apparent speed can be well interpreted by the model, and the intrinsic Lorentz factors of their bulk motion are thus derived. We will adopt the concordant cosmological model (ΛCDM model) with $\Omega_{\rm m} = 0.3$, $\Omega_\Lambda = 0.7$ and Hubble constant $H_0 = 70$ km s^{-1} Mpc^{-1} (Spergel et al. 2003). Thus for 3C 279, $z = 0.538$, its luminosity distance is $D_l = 3.096$ Gpc (Hogg 1999; Pen 1999) and angular diameter distance $D_{\rm a} = 1.309$ Gpc. The angular scale $1\,{\rm mas} = 6.35\,{\rm pc}$ and the proper motion of 1 mas yr^{-1} is equivalent to an apparent velocity of 31.81 c.

2 FORMULISM OF THE MODEL

The formulism and geometry of the precession model have been described in detail in the previous paper (Qian 2011, also see Qian et al. 2009, 1991), referring to its figure 1. Here we only recall the

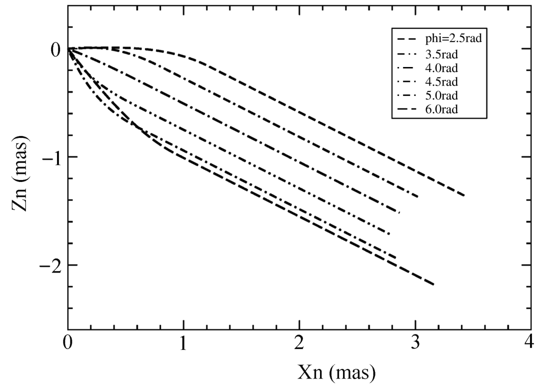

Fig. 1 Distribution of the trajectory depending on the precession phase $\phi = 2.5$, 3.5, 4.0, 4.5, 5.0 and 6.0 rad. Adopted from Qian (2011).

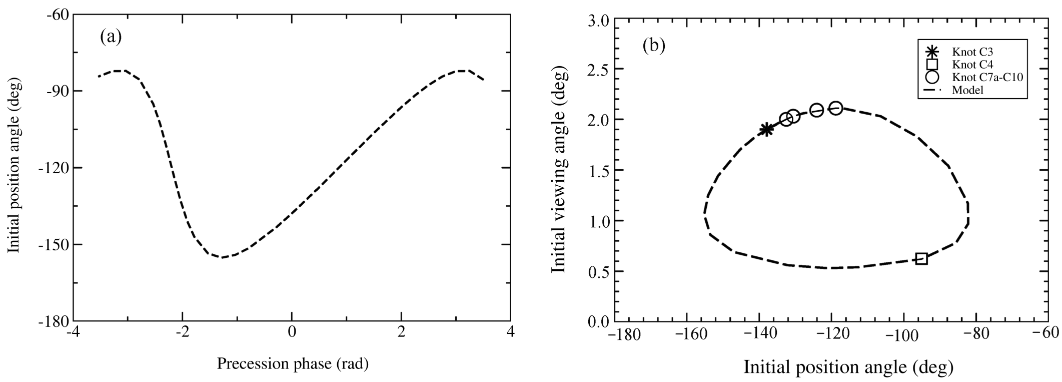

Fig. 2 (a) model relation between the (initial) ejection position angle and the precession phase. (b) model relation between the (initial) ejection position angle and the initial viewing angle (*dashed line*). The precession is in the counterclockwise direction from C3 (*asterisk*), C4 (*square*) to C7a, C8, C9 and C10 (*circles*). See text below.

functional expressions describing the collimated path and the precession phase of the knots (coordinates and amplitude (A) are measured in units of mas). In order to study the initial (ejection) position angle and kinematics of the knots (C3 to C10), we need an appropriate set of model parameters and functions to describe the amplitude and phase of the knots, thus defining their trajectories.

The position of a knot is set by cylindrical coordinates (z, A, Φ): z– distance from the core along the precession axis, A–amplitude of the path and Φ–azimuthal angle. Amplitude (A) as a function of z is taken as:
when $z \leq b$,

$$A(z) = \frac{2b}{\pi} 1.375 \times 10^{-2} \sin\left(\frac{\pi z}{2b}\right), \tag{1}$$

and $z > b$,

$$A(z) = \frac{2b}{\pi} 1.375 \times 10^{-2}, \tag{2}$$

$$\Phi(z) = \text{const.} + \phi, \tag{3}$$

Table 1 Precession model with a period of 25 yr: precession phase ϕ, ejection epoch t_0 and initial position angle (IPA). At epoch 2003.39, precession phase ϕ = 5.0 rad and PA = $-155°$.

ϕ (rad)	t_0 (yr)	IPA (°)	ϕ (rad)	t_0 (yr)	IPA (°)
6.2832	1973.30	−137.9	2.0	1990.35	−96.4
6.0	1974.43	−143.3	1.5	1992.34	−106.4
5.5	1976.42	−151.4	1.0	1994.33	−117.0
5.25	1977.41	−154.1	0.5	1996.32	−127.7
5.0	1978.41	−155.2	0.0	1998.31	−137.9
4.75	1979.40	−153.5	−0.2832	1999.42	−143.3
4.50	1980.40	−147.0	−0.7832	2001.41	−151.4
4.25	1981.39	−133.0	−1.0332	2002.40	−154.1
4.0	1982.39	−112.6	−1.2832	2003.40	−155.2
3.75	1983.38	−95.1	−1.5332	2004.39	−153.5
3.5	1984.38	−85.6	−1.7832	2005.39	−147.0
3.25	1985.37	−82.2	−2.0332	2006.38	−133.0
3.0	1986.37	−82.3	−2.2832	2007.38	−112.6
2.75	1987.36	−84.4	−2.5332	2008.37	−95.1
2.50	1988.36	−87.7	−2.7832	2009.37	−85.6
2.25	1989.35	−91.8	−3.0332	2010.36	−82.2

where const.$= 3.783$ rad (arbitrary) and ϕ is defined to be the precession phase. This form of trajectory represents a collimated jet (knot path).

The formulae for viewing angle θ, apparent transverse velocity β_a and Doppler factor δ and the elapsed time T are given as follows:

$$\theta = \arccos\left[\cos\epsilon(\cos\Delta + \sin\epsilon\tan\Delta_p)\right], \tag{4}$$

$$\delta = \frac{1}{\Gamma(1-\beta\cos\theta)}, \tag{5}$$

$$\beta_a = \frac{\beta\sin\theta}{1-\beta\cos\theta}, \tag{6}$$

$$T = \int_0^z \frac{1+z}{\Gamma\delta v\cos\Delta_s}, \tag{7}$$

where the expressions for Δ, Δ_p and Δ_s are given in Qian (2011).

3 MODEL PARAMETERS AND GENERAL PROPERTIES

In order to model the kinematics of the superluminal knots in the quasar 3C 279 by a precession jet model, our model involves multiple parameters which include the parameters that define the direction of the precession axis and the opening angle of the precession cone, the parameters that define the jet collimation, the shape of the trajectory, the Lorentz factor of the superluminal knots and the precession period (as shown in Qian 2011). Thus we choose some of the appropriate values of the parameters through trial fittings to the kinematic behaviors (apparent trajectories, superluminal speeds and ejection epochs) for as many superluminal knots as possible. Although the set of model parameters chosen is not unique, the results of this paper for the six superluminal knots (C3, C4, C7a, C8, C9 and C10) show that our precession model is appropriate to consistently describe their kinematics.

We have taken parameters $\epsilon = 1.32°$ and $\psi = 28.53°$, which define the direction of the precession axis; $b = 50$ mas and the half opening angle of the precession cone (initial) $\eta = 0.79°$ (from Eq. (1); for details see Qian 2011). With that model we fitted the change in the initial ejection position angle of the superluminal knots with a 25 yr precession period. The general shape of the model trajectory for the knots and their distribution with precession phase (ϕ) is shown in Figure 1 with $b = 50$ mas and $z \leq z_0 = 160$ mas which are chosen mainly for fitting the kinematics of knots C4 and C9.

In Table 1 we summarize the basic properties of the precession model with a period of 25 yr, showing the relationship between the precession phase ϕ (rad), ejection epoch and initial position angle. Figure 1 shows the distribution of the trajectory on the sky-plane with different precession phases. This figure clearly shows the rotation with time of the trajectory of superluminal knots ejected at different times. Figure 2 (a) shows the relation between the precession phase and initial ejection position angle, indicating the asymmetric change with respect to the precession phase for the variation of position angle in the range -82° to -155°. In Figure 2(b) we give the relation between the initial position angle and the initial viewing angle, which shows the change in viewing angle with respect to the position angle. The time is counted along the direction of rotation counterclockwise and the range for viewing angle is $\sim 0.5^\circ$ to 2°. It is obvious that the change in the viewing angle is asymmetric.

Before starting model-fitting to the kinematics, we point out that the fitting quality can be judged by visual inspection, keeping in mind the typical errors in measured position (X_n, Z_n) of $\sim \pm 0.02 - 0.04$ mas, or those in observed core-distance of $\sim \pm 0.03 - 0.08$ mas and in observed position angle of $\sim \pm 5^\circ - 10^\circ$. However, we will show the error bars in the figures for the fitting of apparent speeds with the values given by the relevant VLBI-measurements.

4 MODEL-FITTING TO THE KINEMATICS OF KNOTS

We will study the model-fitting of the kinematics (trajectory, core-distance and apparent velocity) of the knots C3, C4, C7a, C8, C9 and C10. We begin with knot C4.

4.1 Knot C4

Superluminal component C4 has been studied by Cotton et al. (1979), Unwin et al. (1989), Carrara et al. (1993), Abraham & Carrara (1998), Wehrle et al. (2001) and Homan et al. (2003). A detailed analysis of its kinematics was given by Homan et al. (2003), who found that the trajectory of component C4 was along a position angle $\sim -114^\circ$ with an apparent velocity 7.9c±0.6c prior to ∼1998.2 and after ∼ 1998.2 it approached along a position angle $\sim -140^\circ$ with an apparent velocity of 12.7c±0.3c. Although this recollimation process occurred gradually, as shown by Jorstad et al. (2005), we simply use a broken linear form to describe its trajectory in the model-fitting. Taking into account the available observational results given by the authors listed above, we adopt the ejection epoch of C4 to be $t_0 = 1983.4$ [1] and its apparent velocity β_a to be 7.9c±0.6c (prior to 1998.2) and 12.7c±0.3c (after 1998.2).

Since the trajectory of knot C4 has significant curvature at a core-distance of ∼3 mas, we have to describe its trajectory beyond this core-distance using a different expression. As shown in the previous paper (Qian 2011), corresponding to this ejection time, the precession phase for C4 is $\phi = 3.75$ rad and its trajectory can be well fitted by a model amplitude function presented in Figure 3(a): for $z \leq z_0 = 160$ mas the model amplitude is given by Equations (1) and (2), and for $z > z_0 = 160$ mas the amplitude function is given by (see Qian 2011)

$$A(z) = \frac{2b}{\pi}(1.375 \times 10^{-2})\big[1 - (z - 160)/10\big]\,. \tag{8}$$

[1] We point out that the ejection epoch determined by different authors for C4 is quite different: 1984.7±0.3 (Wehrle et al. 2001; Homan et al. 2003); 1981.4 (Carrara et al. 1993); 1981.0±1 (Abraham & Carrara 1998). We chose a more appropriate value: 1983.4 as the fit-results show.

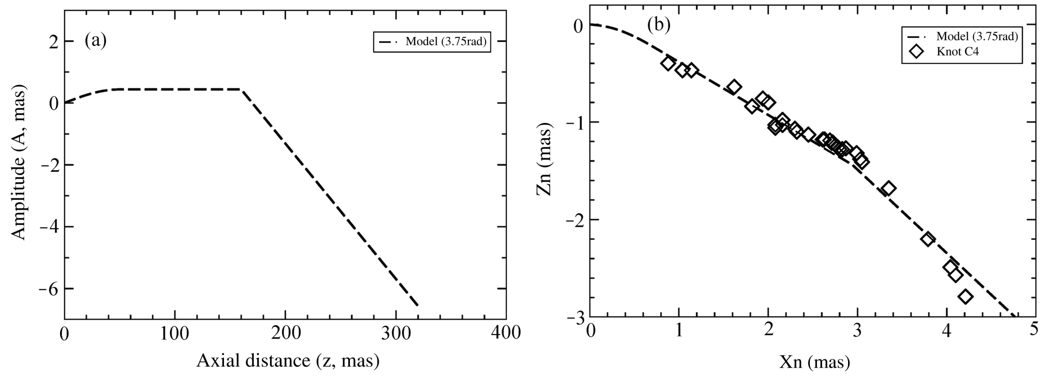

Fig. 3 Model amplitude function (a) and model-fitting to the observed trajectory (b) for knot C4.

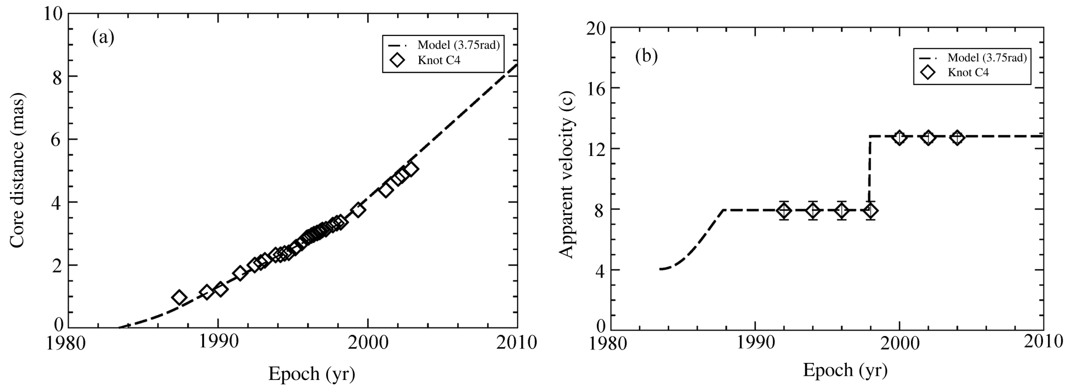

Fig. 4 Model-fitting to the observed core distance (a) and apparent velocity (b) of knot C4.

Thus correspondingly, the initial ejection PA = $-95.1°$ and the knot approaches towards $-114°$ at core-distances larger than 3 mas, as observed. The fits to the trajectory and core-distance are shown in Figure 3(b) and Figure 4(a) respectively. Both are very good (taken from Qian 2011).

In order to fit the apparent motion of knot C4 we have to choose the value for the bulk Lorentz factor $\Gamma = 13.8$ at axial-distance $z \leq 160$ mas and 13.0 at $z > 160$ mas. Since these parameters were chosen, the kinematics of the knot were calculated. Figure 4(b) shows the model-fitting to the observed apparent velocity. It can be seen that the apparent velocity β_a is very well fitted. The model Lorentz/Doppler factor and model viewing angle are shown in Figure 5. We also note that the slight change of its apparent velocity (from $\sim 8\,c$ to $13\,c$, as required by VLBI observations, Homan et al. 2003) can be fitted by the increase in viewing angle (from $1.3°$ to $3.8°$) and a slight decrease in bulk Lorentz factor from 13.8 to 13.0 (the curvature occurs at core-distance $\sim$3 mas, corresponding to deprojected distance $\sim$160 mas, or $\sim$1 kpc from the core (1 mas = 6.35 pc). The Doppler factor decreases from $\sim$26 (core-distance <3 mas) to $\sim$15 (core-distance >3 mas), which is very consistent with the analysis of Homan et al. (2003) for its kinematics.

Our model-fitting results are very consistent with those derived by Homan et al. (2003), in which the kinematics of knot C4 were analyzed in detail for the period 1996–2002. They estimated the bulk Lorentz factor of C4 $\Gamma \geq 15$ with an initial angle to the line of sight of $\theta \leq 1°$, increasing at the bend to become $\theta \leq 2°$. This bend in the plane of the sky appears to be $\sim 26°$, but deprojected this bend is only $\sim 0.5°$– $1°$. They also found that the averaged motions were (7.9±0.6)c prior to $\sim$1998.2 and (12.7±0.3)c after $\sim$1998.2 and derived approximate limits on the Doppler beaming factor: $\delta \geq 28$

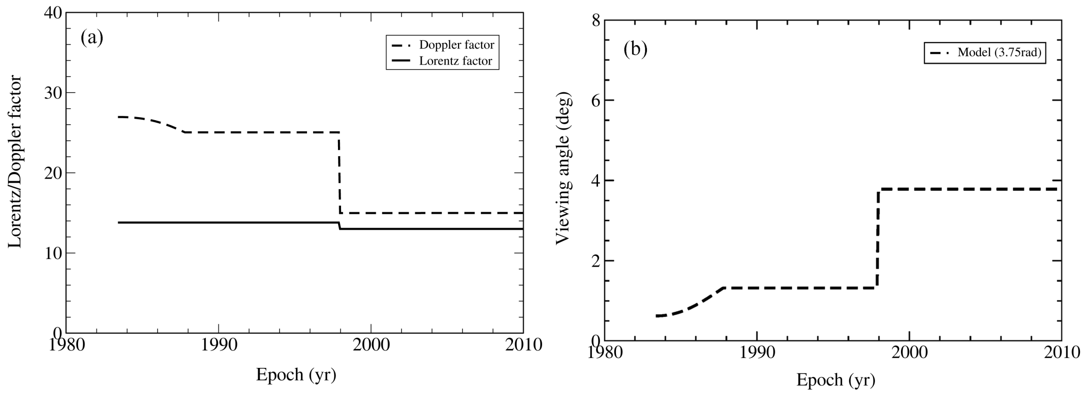

Fig. 5 Model bulk Lorentz/Doppler factor (a) and model viewing angle (b). The bulk Lorentz factor is taken to be $\Gamma = 13.8$ ($z \leq 160$ mas) and $\Gamma = 13.0$ ($z > 160$ mas), $t_0 = 1983.4$. Precession phase = 3.75 rad.

prior to the change in trajectory and $\delta \geq 23$ after the change. Regarding the change in the trajectory, Homan et al. (2003) suggested that C4 has been deflected onto its new trajectory. The change in trajectory is a collimation event resulting from the interaction of C4 with the boundary between the jet flow and the interstellar medium. The exact nature of this boundary and interaction is unclear.

In summary, we can see that the fitting of kinematic properties for knot C4 is remarkable. All the features (including its entire trajectory, core-distance variation, changes in apparent velocity, viewing angle and Doppler factor) are consistently well fitted by the precession jet model with parameter $b = 50$ mas and amplitude function given by Equations (1) and (2), which are proposed in our previous paper (Qian 2011). Furthermore, both the initial position angle and initial ejection epoch we used are consistent with the precession period of 25 yr, as shown in Qian (2011). Thus the successful model-fitting to knot C4 makes us more confident of the applicability of the model. It also demonstrates that the trajectory of C4 needs to be described by both a first collimation (at distance $b = 50$ mas) and a gradual curvature (at $\sim$160 mas). This feature could be significant in understanding the kinematics of the superluminal components in 3C 279. For example, if this kind of curvature occurs at much smaller distances (e.g. axial distance $z \ll 50$ mas), then the resulting trajectory near the core would be very different from that given by the current model.

In particular, we emphasize that the change in viewing angle derived for C4 is consistent with Homan et al. (2003). This demonstrates the applicability of our precession model with small viewing angles. This is consistent with other kinematic properties of 3C 279 (e.g. the Doppler factor, Lorentz factor and superluminal motion measured for other knots, and also variability properties (in gamma-ray, X-ray, optical and mm-radio radiation)).

4.2 Model-fitting of the Kinematics of Knot C3

Knot C3 is the earliest ejected component used in this paper and was ejected ten years before C4. Its fit by the model is significant for testing the precession period. The data are from Homan et al. (2003), Unwin et al. (1989) and Carrara et al. (1993).

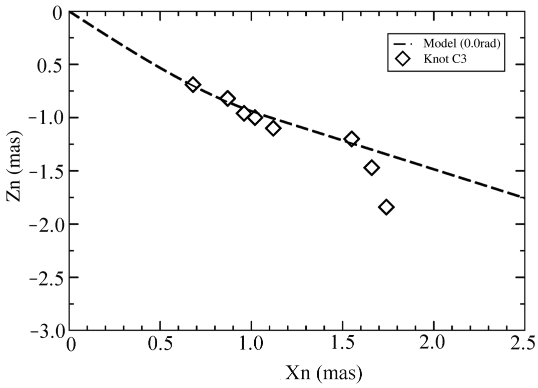

Fig. 6 Model-fit to the observed trajectory of knot C3.

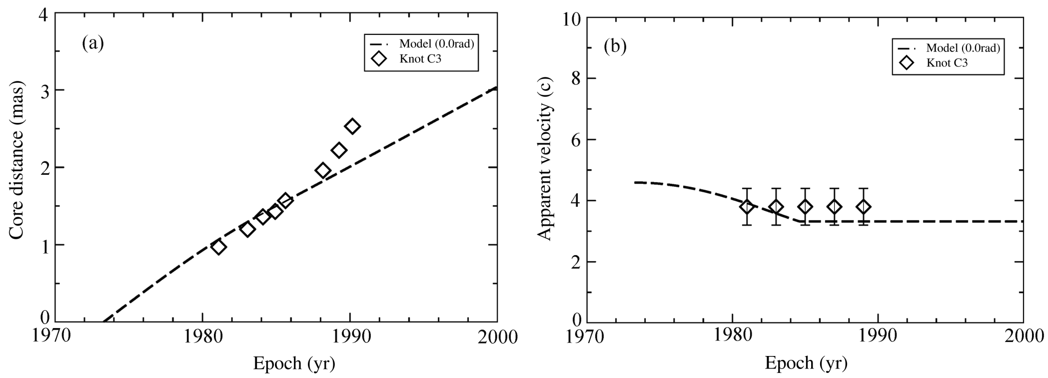

Fig. 7 Model-fits to the core-distance (a) and apparent velocity (b) of knot C3. $\Gamma = 8.7$, precession phase $\phi = 0.0$ rad, $t_0 = 1973.3$.

We adopt the ejection epoch $t_0 = 1973.3$[2], $\Gamma = 8.7$, the corresponding precession phase $\phi = 0.0$ rad, the initial viewing angle $= 1.9°$ and initial position angle (ejection angle)$= -137.9°$.

The fitting results for knot C3 are shown in Figures 6–8. It can be seen from Figure 6 and Figure 7(a) that the fits to the trajectory and core-distance are very good for the period between 1980 and 1989, with only the last two observational points apparently deviating from the model (at core-distance >2 mas). The apparent velocity of its superluminal motion ($\beta_a = 4 \pm 1$, given by Homan et al. 2003) is also fitted very well, as shown in Figure 7(b). Figure 8 shows that its viewing angle in the period from 1980 to 1989 is about $\sim 1.3°$ and the Doppler factor is ~ 16.

4.3 Model-fitting of the Kinematics of Knot C7a

The knot C7a data are taken from Wehrle et al. (2001) and Jorstad et al. (2004). We adopt $t_0 = 1994.67$, the corresponding precession phase $\phi = 0.915$ rad and observed apparent velocity $\beta_a = 5.0 \pm 0.3$. The bulk Lorentz factor is taken to be $\Gamma = 8.9$ (similar to C3). The initial viewing angle is $2.11°$ and ejection position angle (initial PA) is $-118.8°$.

[2] We point out that in the literature the published ejection epoch determined for C3 by different authors is quite different: 1976.2±1 (Abraham & Carrara 1998); 1972.6±1.1 (Unwin et al. 1989; Homan et al. 2003). We adopt $t_0 = 1973.3$, which is a more appropriate value as the model-fitting shows.

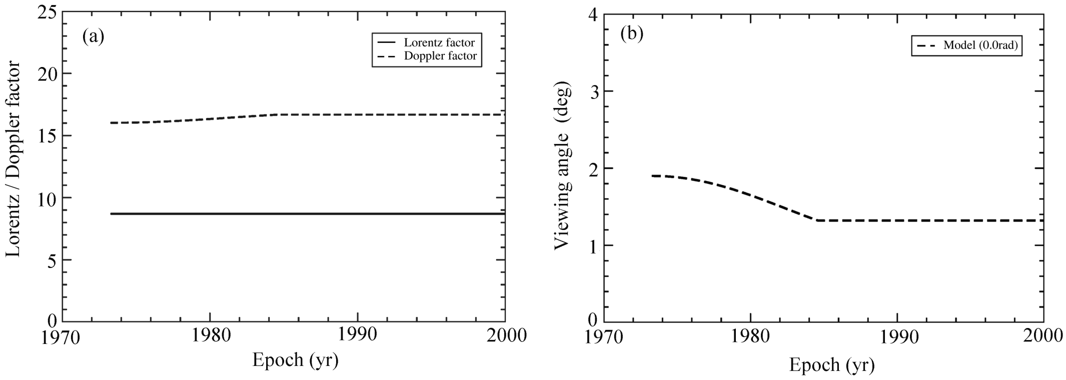

Fig. 8 Model bulk Lorentz/Doppler factor (a) and model viewing angle (b) for knot C3.

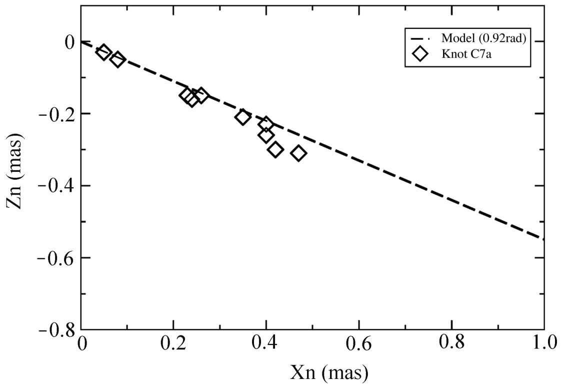

Fig. 9 Model fit to the observed trajectory of knot C7a.

The fitted results are shown in Figures 9–11. It can be seen from Figures 9 and 10(a) that both the trajectory and the core-distance are well fitted, especially for the points with core-distances less than 0.5 mas. In Figure 10(b) its apparent velocity is fitted very well ($\beta_a = 5.0 \pm 0.3$, Jorstad et al. 2004). Figure 11 shows that knot C7a has a larger initial viewing angle ($\sim$2.11°).

The significant features are: (1) the observed trajectory in the core-distance range of less than 0.1 mas is well situated on the model curve, showing the correctness of the precession period (25 yr) and $b = 50$ mas (collimation parameter) is well applied near the core (at core-distance <0.4 mas). This strengthens the applicability of the model at small core-distances. (2) However, at larger core distances the observed trajectory slightly deviates from the model one, which could be explained by interactions between the knot and its environment. In this case the interaction could occur at radial distance $z = 80$ mas. This phenomenon has already been seen in the case of knot C4. The Doppler factor is derived to be $\sim$16 (Fig. 11(a)), similar to knot C3.

4.4 Model-fitting of the Kinematics of Knot C8

Data are taken from Wehrle et al. (2001), Jorstad et al. (2004) and Chatterjee et al. (2008). For knot C8 we adopt ejection epoch 1995.63. The corresponding precession phase is $\phi = 0.667$ rad and thus the initial viewing angle is 2.09° and the ejection position angle is $-124.1°$. The observed apparent

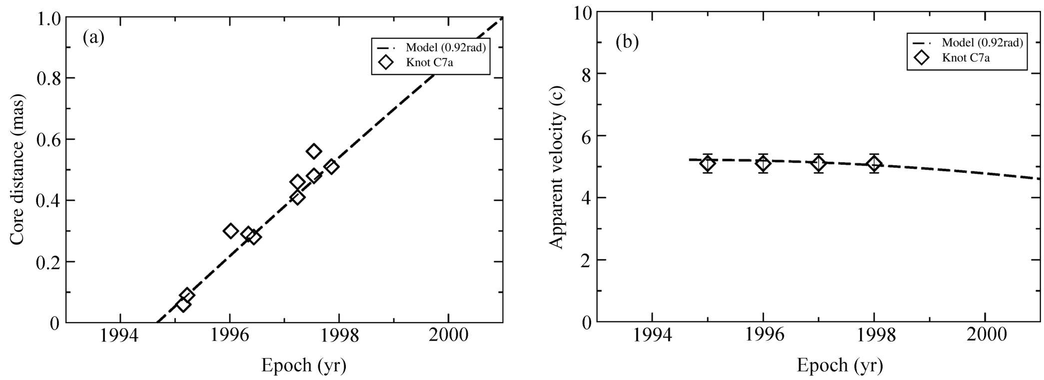

Fig. 10 Model-fits to the core-distance (a) and apparent velocity (b) for knot C7a. Bulk Lorentz factor $\Gamma = 8.9$, ejection epoch $t_0 = 1994.67$ and precession phase $\phi = 0.92$ rad.

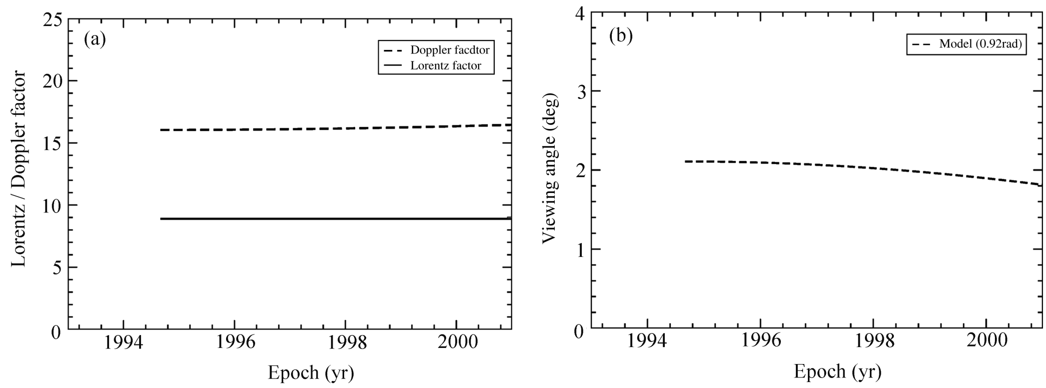

Fig. 11 Model bulk Lorentz/Doppler factor (a) and model viewing angle (b) for knot C7a.

velocity is taken to be $\beta_a = 5.4 \pm 0.7$. We assume bulk Lorentz factor $\Gamma = 9.2$. The fitting results are shown in Figures 12–14.

The fittings for the trajectory and core-distance are marginally good (Figs. 12 and 13(a)), considering the errors in the observed position of the knot (typically, $\sim \pm 0.02 - 0.04$ mas and in observed position angle $\sim\pm 5°$–$10°$). The apparent velocity is fitted well, as shown in Figure 13(b).

The data taken from the literature are for core-distances less than ∼0.4 mas, which helps to check the applicability of the model to the initial ejection behavior very near the core (similar to the case for knot C7a). It can be seen that all the observed trajectory, apparent velocity and core-distance variations with time are well fitted in this core-distance range. For the ejection time we adopted the value inferred by Wehrle et al. (2001) and Jorstad et al. (2004), thus its motion can be well fitted to core-distance ∼0.4 mas, as shown in Figures 12 and 13. The fit to the observed superluminal motion is remarkably good (Fig. 13(b)). [3] Figure 14 shows the model Lorentz/Doppler factor and the model viewing angle. The Doppler factor $\delta =\sim 16.5$ and the viewing angle $\theta =\sim 2.1°$ in 1996–1998.

[3] Different VLBI observers give different ejection times, ejection position angles and apparent velocity. For example, $t_0 = 1995.70$ (Jorstad et al. 2004), $t_0 = 1995.63$ (Wehrle et al. 2001), $t_0 = 1996.09$ (Chatterjee et al. 2008), and their errors in these parameters are also different. This raises some problems in model fitting, because $\Delta t_0 = 0.25$ yr would cause $\Delta\phi = 0.063$ rad, producing a significant change in the model-fitting of the apparent trajectory.

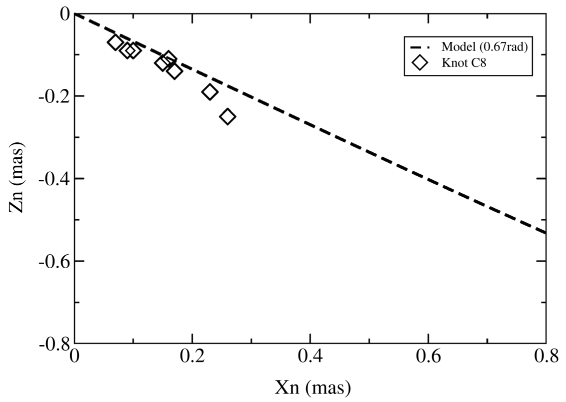

Fig. 12 Model fit to the observed trajectory of knot C8.

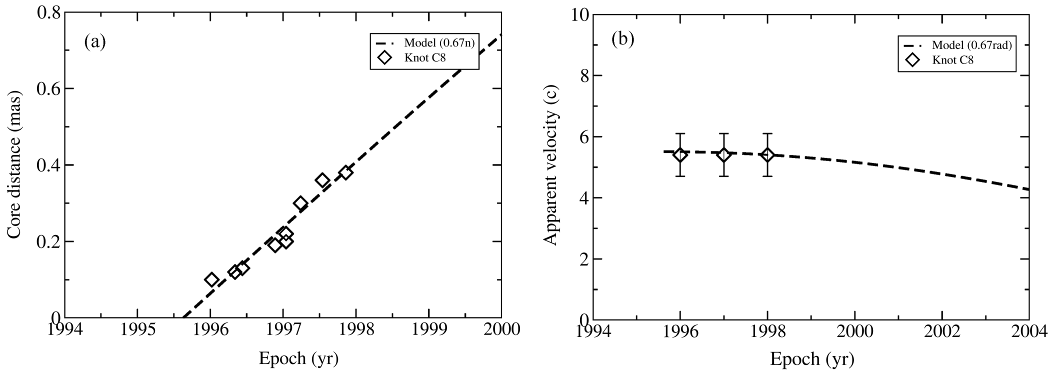

Fig. 13 Model-fits to the core-distance (a) and apparent velocity (b) of knot C8. Ejection epoch $t_0 = 1995.63$, bulk Lorentz factor $\Gamma = 9.2$ and precession phase $\phi = 0.67$ rad.

4.5 Model-fitting of the Kinematics of Knot C9

Data are taken from Jorstad et al. (2004) and Chatterjee et al. (2008). We adopt ejection time (epoch) $t_0 = 1996.89$, observed apparent velocity $\beta_a = 12.9 \pm 0.3$ (Jorstad et al. 2004; Chatterjee et al. 2008) and corresponding precession phase $\phi = 0.36$ rad. Thus the initial (ejection) position angle is -130.6° and initial viewing angle is 2.03°. In the model-fitting we take bulk Lorentz factor $\Gamma = 16.0$. The fitting results are shown in Figures 15–17.

It can be seen from Figure 15 and Figure 16(a) that the trajectory and core-distance are well fitted by the model between core-distance ∼0.2 mas and ∼1.7 mas (corresponding to a deprojected radial distance from ∼6 mas to ∼50 mas, or ∼38 pc to ∼0.3 kpc). Combining with the fitting to the trajectory of knot C4, we unexpectedly find that our model is applicable to trajectory-fitting from near the core to 2–3 mas (note the precession phases of C4 and C9 differ by about 3.4 rad, i.e. half of the precession period in time). The observed apparent velocity $\beta_a = 12.9 \pm 0.3$ is also well fitted, using bulk Lorentz factor $\Gamma = 16.0$ (Fig. 16(b)). All these imply that our precession model with a period of 25 yr and with a collimation parameter $b = 50$ mas and amplitude function (Eqs. (1) and (2)) is very appropriate to apply to quasar 3C 279.

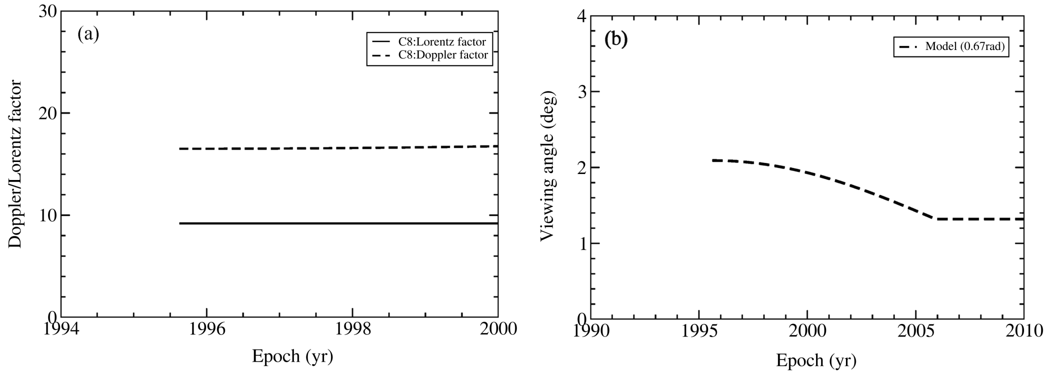

Fig. 14 Model Lorentz/Doppler factor (a) and model viewing angle (b) for knot C8.

Table 2 Model parameters for the six knots: ejection time t_0, precession phase ϕ, bulk Lorentz factor (Γ), initial position angle (IPA), initial viewing angle (IVA) and position angle measured by VLBI ($\mathrm{PA_{VLBI}}$).

Knot	t_0	ϕ (rad)	Γ	IPA ($^\circ$)	IVA ($^\circ$)	$\mathrm{PA_{VLBI}}$ ($^\circ$)
C3	1973.3	6.28	8.7	–137.9	1.90	-134 ± 10 (Unwin et al. 1989)
C4	1983.4	3.75	13.8/13.0	–95.1	0.62	-114 ± 1 (Wehrle et al. 2001)
C7a	1994.67	0.92	8.9	–118.8	2.11	-121 ± 2.1 (Jorstad et al. 2004)
C8	1995.63	0.67	9.2	–124.1	2.09	-130 ± 3 (Chatterjee et al. 2008)
C9	1996.89	0.36	16.0	–130.6	2.03	-131 ± 5 (Chatterjee et al. 2008)
C10	1997.24	0.27	14.0	–132.5	2.00	-132 ± 6 (Chatterjee et al. 2008)

It can be seen from Figure 17 that its ejection viewing angle is 2° and approaches 1.3° at a larger core distance, i.e. its trajectory curves towards the line of sight.

4.6 Model-fitting of the Kinematics of Knot C10

Data are taken from Jorstad et al. (2004) and Chatterjee et al. (2008). We adopt $t_0 = 1997.24\pm0.16$.[4] The corresponding precession phase is 0.27 rad. We take the observed apparent velocity β_a=9.9±0.5. [5] We take the bulk Lorentz factor $\Gamma = 14.0$. Thus the initial position angle is -132.5° and initial viewing angle is 2.0°.

The fitting results are shown in Figures 18–20. It can be seen from Figure 18 and Figure 19(a) that in the range of core-distance between ∼0.2 mas and ∼0.8 mas, the trajectory and core-distance can be well fitted, but at core-distance larger than ∼0.8 mas, the trajectory deviates from the model trajectory, which could be a phenomenon similar to that seen in knot C4 due to some sort of interaction between the jet and the interstellar environment. However, the fit to the trajectory within a core-distance less than ∼1.0 mas is still remarkable. The observed apparent velocity is also very well fitted (Fig. 19(b)). This implies that our model with a 25 yr period and the collimation parameter $b = 50$ mas is successful.

The model Lorentz/Doppler factor and model viewing angle are shown in Figure 20. The Doppler factor for this knot is ∼22 and its viewing angle is about 2°–1.8° in 1998–2001. Thus the kinematics of knot C10 can also be well fitted by the same precession model (Qian 2011).

[4] Jorstad et al. (2004) gives $t_0 = 1997.42$. We adopt the value given by Chatterjee et al. (2008).

[5] Jorstad et al. (2004) gives $\beta_a = 8.5 \pm 1.6$. We adopt the value from Chatterjee et al. (2008).

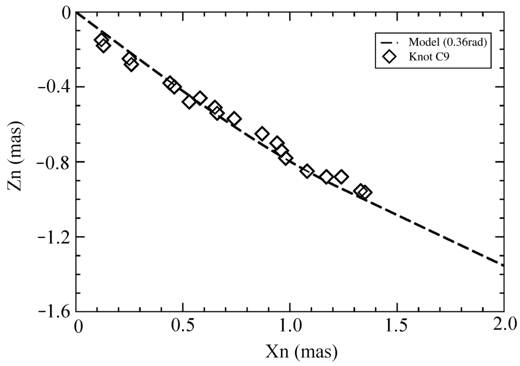

Fig. 15 Model-fit to the observed trajectory of knot C9.

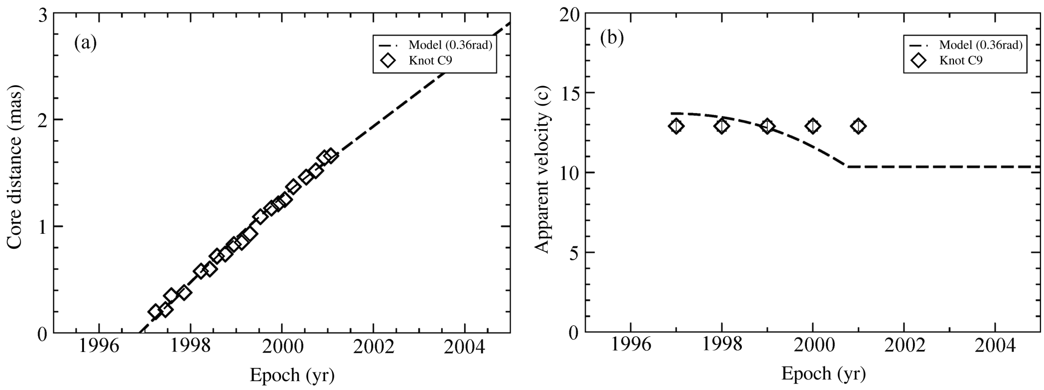

Fig. 16 Model-fits to the core distance (a) and apparent velocity (b) of knot C9. $\Gamma = 16.0$, $t_0 = 1996.89$ and $\phi = 0.36\,\mathrm{rad}$.

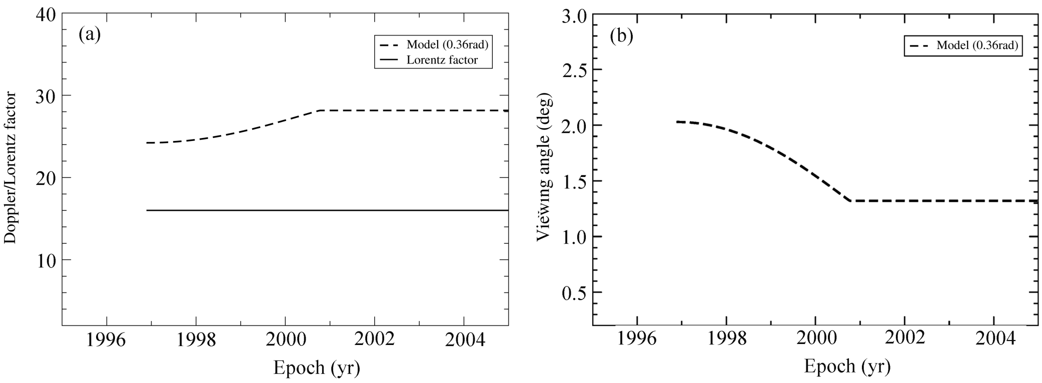

Fig. 17 Model Lorentz/Doppler factor (a) and model viewing angle (b) for knot C9.

5 DISCUSSION AND CONCLUSION

We summarize the model-fitting parameters (ejection time t_0, precession phase ϕ, bulk Lorentz factor Γ, initial position angle and initial viewing angle) for the six superluminal components (C3,

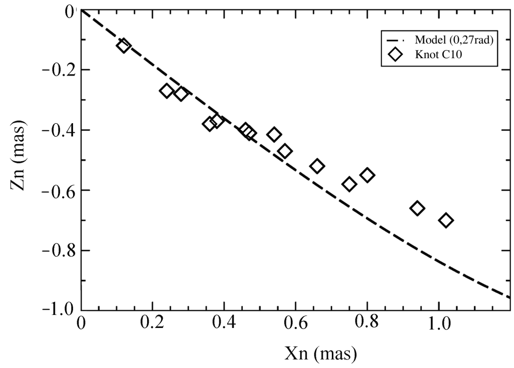

Fig. 18 Model-fit to the observed trajectory of knot C10.

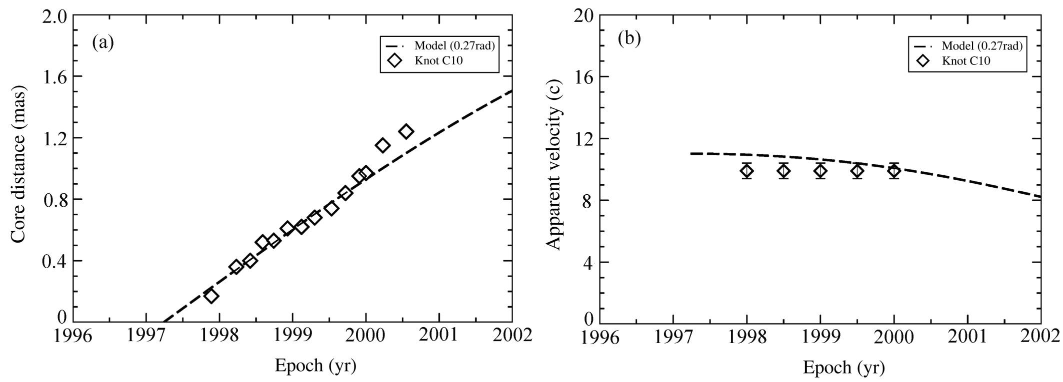

Fig. 19 Model-fits to the core distance (a) and apparent velocity (b) of knot C10. Ejection epoch $t_0 = 1997.24$, Lorentz factor $\Gamma = 14.0$, precession phase $\phi = 0.27$ rad.

C4, C7a, C8, C9 and C10) in Table 2. The comparison between the initial position angles derived by the model and those given by VLBI observations shows that they are consistent within $3° - 6°$ (except for knot C4).

From Figures 3 to 20 it can be seen that the fitting results for the trajectory, core-distance and apparent speed are good for all six knots. Although the ejection epochs of knots C9 and C10 are separated in time from that of knot C4 by about 13–14 yr (or one half of the precession period), they are well fitted by the same trajectory pattern. This implies that not only the ejection direction but also their trajectory can be obtained by rotation of a stable channel. In addition, the fittings to the apparent speeds are very impressive. The values given by the model deviate from those given by VLBI measurements by less than 10% to 15%.

Some authors have suggested that the different apparent superluminal velocities observed for different knots in 3C 279 could be caused by the precession of the jet with constant Lorentz factor. We have obtained (for the six superluminal knots fitted in this paper) the relation between the ejection bulk Lorentz factor and ejection position angle, which is shown in Figure 21. It does not show any regular trend in the bulk Lorentz factor. Since these Lorentz factor values are derived from the model-fitting to the trajectories, core-distances and apparent speeds observed by VLBI observations, they should be regarded as very determined (with errors at most $\pm 20\%$). It seems that the observed apparent speed is not simply dependent on the precession-produced change in the viewing angle

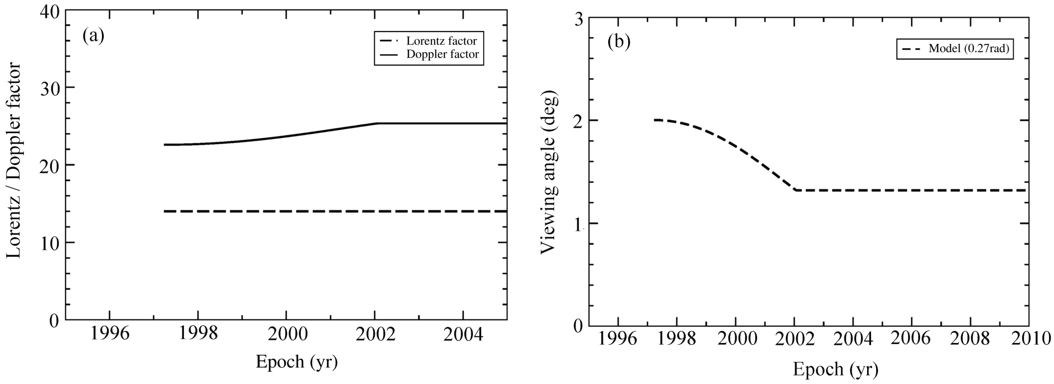

Fig. 20 Model Lorentz/Doppler factor (a) and model viewing angle (b) for knot C10.

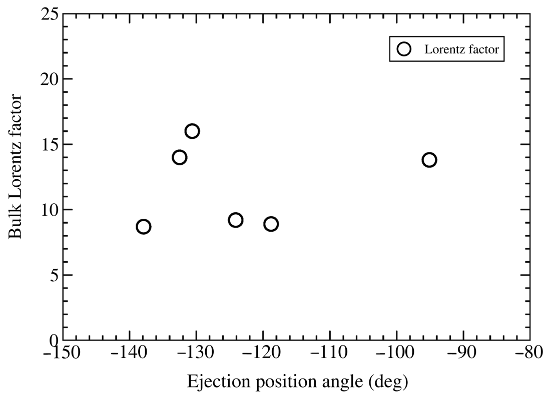

Fig. 21 Relation between bulk Lorentz factor and ejection position angle for knots C3 to C10, showing no clear trend.

with a constant Lorentz factor. In other words, the bulk Lorentz factor of knots could depend on the activity in the central black hole/accretion system, and the efficiency of the energy transfer to the jet, which could vary non-regularly. From the fitting results for knots C3, C4, C7a, C8, C9 and C10, we can see that their trajectory, core-distance, apparent velocity and ejection position angle are all well fitted by the precession model proposed in our previous paper (Qian 2011) with the common model-parameters for the collimation parameter ($b = 50$ mas) and amplitude function given by Equations (1)–(2). We note that on a physical basis our precession model of a collimated jet described by these equations is quite simple, but it seems remarkable that the kinematics of these knots, spanning a long ejection time interval (1973.3 (C3) to 1997.24 (C10)), can be consistently well explained. This might show that the VLBI structure is really solid and stable during this period. We will show that more superluminal components can be well fitted by our precession model in a future paper.

It is worth summarizing the core-distance ranges in which the kinematics of the six knots are well fitted as follows:

Knot C3: from $\sim$1 to $\sim$2 mas;
Knot C4: from $\sim$1 to $\sim$3 mas (before the curvature at 1998.2);

Knot C9: from ∼0.2 to ∼1.5 mas;
Knot C7a: from ∼0.05 to ∼0.5 mas;
Knot C8: from ∼0.1 to ∼0.3 mas;
Knot C10: from ∼0.2 to ∼0.8 mas.

Thus our jet-precession model with a period of 25 yr is applicable to consistently fit the kinematics of these knots for the core-distance ranging between ∼0.1 mas and ∼1.5–2 mas (i.e. for both small and large core distances and time spans of one period).

The fits to those for knot C4 can be regarded as a representative example to show how the model is applied to study the kinematics of superluminal knots in 3C 279. Its trajectory derived from the precession model can well fit the VLBI observation before 1998.2 (its precession phase and corresponding ejection position angle are derived from its ejection time) and the inclusion of the curvature of its trajectory can well explain the observed change in trajectory and apparent velocity after 1998.2. Moreover, the good fit to the kinematic behavior of knot C9 in the range of core-distance ∼0.2–1.6 mas (Figs. 15–16) demonstrates that our model is applicable to describe its kinematics in both the inner region (within core-distance ∼0.2 mas) and the outer region.

Finally, we indicate that our model includes three crucial ingredients: (1) precession of the jet; (2) collimation near the core; and (3) curvature of trajectory in the outer region. If different parameters were chosen for defining these ingredients, this would lead to both different behaviors of kinematics and different distributions of trajectory.

Undoubtedly, the consistent interpretation of the kinematics of all six superluminal knots in terms of the precession model expands the applicability of the model (besides accounting for the jet-nozzle precession) and implies that some regular pattern of trajectory (or a rotating channel) could exist in certain periods. This kind of steady rotating channel, if it really exists, must be strongly related to the magnetic structure of the central engine (Meier & Nakamura 2006; McKinney 2006; Vlahakis & Königl 2004; Meier 2001; Meier et al. 2001). Jet precession could be related to binary black hole systems as one of the mechanisms (Britzen et al. 2001; Karouzos et al. 2011; Kudryavtseva et al. 2011).

References

Abdo, A. A., Ackermann, M., Agudo, I., et al. 2010, ApJ, 716, 30
Abraham, Z., & Carrara, E. A. 1998, ApJ, 496, 172
Agudo, I., Jorstad, S. G., Marscher, A. P., et al. 2011, ApJ, 726, L13
Britzen, S., Roland, J., Laskar, J., et al. 2001, A&A, 374, 784
Carrara, E. A., Abraham, Z., Unwin, S. C., & Zensus, J. A. 1993, A&A, 279, 83
Chatterjee, R., Jorstad, S. G., Marscher, A. P., et al. 2008, ApJ, 689, 79
Cohen, M. H., Cannon, W., Purcell, G. H., et al. 1971, ApJ, 170, 207
Cotton, W. D., Counselman, C. C., III, Geller, R. B., et al. 1979, ApJ, 229, L115
Hartman, R. C., Bertsch, D. L., Fichtel, C. E., et al. 1992, ApJ, 385, L1
Hogg, D. W. 1999, arXiv:astro-ph/9905116
Homan, D. C., Lister, M. L., Kellermann, K. I., et al. 2003, ApJ, 589, L9
Jorstad, S. G., & Marscher, A. P. 2005, Mem. Soc. Astron. Italiana, 76, 106
Jorstad, S. G., Marscher, A. P., Larionov, V. M., et al. 2010, ApJ, 715, 362
Jorstad, S. G., Marscher, A. P., Lister, M. L., et al. 2004, AJ, 127, 3115
Jorstad, S. G., Marscher, A. P., Lister, M. L., et al. 2005, AJ, 130, 1418
Jorstad, S. G., Marscher, A. P., Stevens, J. A., et al. 2007, AJ, 134, 799
Karouzos, M., Britzen, S., Witzel, A., Zensus, J. A., & Eckart, A. 2011, A&A, 529, A16
Kudryavtseva, N. A., Britzen, S., Witzel, A., et al. 2011, A&A, 526, A51
Larionov, V. M., Jorstad, S. G., Marscher, A. P., et al. 2008, A&A, 492, 389

Marscher, A., Jorstad, S. G., Larionov, V. M., Aller, M. F., & Lähteenmäki, A. 2011, Journal of Astrophysics and Astronomy, 32, 233 (arXiv: 1101.0179)

Marscher, A. P. 2008, in Astronomical Society of the Pacific Conference Series 386, Extragalactic Jets: Theory and Observation from Radio to Gamma Ray, eds. T. A. Rector & D. S. De Young, 437

Marscher, A. P. 2009, in Astronomical Society of the Pacific Conference Series 402, Approaching Micro-Arcsecond Resolution with VSOP-2: Astrophysics and Technologies, eds. Y. Hagiwara, E. Fomalont, M. Tsuboi, & M. Yasuhiro, 194

Marscher, A. P., & Jorstad, S. G. 2011, ApJ, 729, 26

Marscher, A. P., Jorstad, S. G., Larionov, V. M., et al. 2010, ApJ, 710, L126

McKinney, J. C. 2006, MNRAS, 368, 1561

Meier, D. L. 2001, ApJ, 548, L9

Meier, D. L., Koide, S., & Uchida, Y. 2001, Science, 291, 84

Meier, D. L., & Nakamura, M. 2006, in Astronomical Society of the Pacific Conference Series 350, Blazar Variability Workshop II: Entering the GLAST Era, eds. H. R. Miller, K. Marshall, J. R. Webb, & M. F. Aller, 195

Pen, U.-L. 1999, ApJS, 120, 49

Qian, S.-J. 2011, RAA (Research in Astronomy and Astrophysics), 11, 43

Qian, S. J., Krichbaum, T. P., Zensus, J. A., Steffen, W., & Witzel, A. 1996, A&A, 308, 395

Qian, S. J., Witzel, A., Krichbaum, T., et al. 1991, Acta Astronomica Sinica, 32, 369 (English translation: in Chin. Astro. Astrophys. 1992, 16, 137)

Qian, S.-J., Witzel, A., Zensus, J. A., et al. 2009, RAA (Research in Astronomy and Astrophysics), 9, 137

Raiteri, C. M., Villata, M., Bruschini, L., et al. 2010, A&A, 524, A43

Schinzel, F. K., Lobanov, A. P., Jorstad, S. G., et al. 2010, In Fermi meets Jansky – AGN in Radio and Gamma-Rays, eds. T. Savolainen, E. Ros, R. W. Porcas, & J. A. Zensus, 175 (arXiv: 1012.2820)

Spergel, D. N., Verde, L., Peiris, H. V., et al. 2003, ApJS, 148, 175

Steffen, W., Zensus, J. A., Krichbaum, T. P., Witzel, A., & Qian, S. J. 1995, A&A, 302, 335

Unwin, S. C., Cohen, M. H., Hodges, M. W., Zensus, J. A., & Biretta, J. A. 1989, ApJ, 340, 117

Vercellone, S., D'Ammando, F., Vittorini, V., et al. 2010, ApJ, 712, 405

Vlahakis, N., & Königl, A. 2004, ApJ, 605, 656

Wehrle, A. E., Piner, B. G., Unwin, S. C., et al. 2001, ApJS, 133, 297

Whitney, A. R., Shapiro, I. I., Rogers, A. E. E., et al. 1971, Science, 173, 225